Science Advances
AAAS

Supplementary Materials for

Polygenic risk for alcohol use disorder affects cellular responses to ethanol exposure in a human microglial cell model

Xindi Li *et al.*

Corresponding author: Zhiping P. Pang, pangzh@rwjms.rutgers.edu

Sci. Adv. **10**, eado5820 (2024)
DOI: 10.1126/sciadv.ado5820

This PDF file includes:

Supplementary Text

Full details of **bioinformatics analysis of RNA-Seq data**

Data processing and normalization

We normalize the sample x gene count matrix using the log (counts per million mapped reads) method. In detail, we denote r_{ij} as our matrix of raw read counts, for samples $j \in \{1, \ldots, 9\}$, and genes $i \in \{1, \ldots, G\}$. For sample j, we calculate its total number of mapped reads: $R_j = \sum_{i=1}^{G} r_{ij}$.

Next, we calculate the log-counts per million (log-CPM) value for each gene in each sample as: $y_{ij} = \log_2\left(\frac{r_{ij}+0.5}{R_j+1.0} \times 10^6\right)$.

The normalized data (y_{ij}) are then subject to subsequent analyses.

Differential expression analyses

We use the *limma+voom method (98, 99)* to model the normalized expression level of genes. On the whole, our pipeline consists of three steps: 1) linear modeling *(99)*, 2) *voom* variance modeling, and 3) empirical Bayes differential expression analysis.

First, for linear modeling, we consider a nested interaction formula due to the multiple grouping factors in this study: $y \sim 0 + PRS{:}\,Concentration + PRS{:}\,CellLine$, where y_{ij} represents the normalized gene expression. Next, we assume that: $E(y_{ij}) = \mu_{ij} = x_j\beta_i$, where x_j represents the vector of grouping factors aforementioned for sample j, and β_i represents the coefficient of gene i that represents the log2-fold-changes (log2FC) in expression between the grouping factors.

Second, we estimate the mean-variance relationship of the gene log-counts so that we obtain the precision weights of genes. In detail, we calculate the fitted counts: $E(r_{ij}) = E(\mu_{ij}) + \log_2(R_j + 1) - \log_2(10^6)$, where $E(\mu_{ij})$ stands for fitted log-CPM values, which is calculated using the linear regression coefficient estimates β_i and covariates x_j. Next, to retain a smooth mean-variance trend, we fit a LOWESS curve *(100)* to the square-root of residual standard deviations obtained from the linear model as a function of mean log-counts across all samples. Therefore, we can calculate the precision weights:

$$\omega_{ij} = lo\left(E(r_{ij})\right)$$

where $lo(\cdot)$ represents the piecewise linear function defined by the LOWESS curve.

Finally, the log-CPM values y_{ij} and their associated weights w_{ij} are then subject to the *limma* standard linear modeling and empirical-Bayes-based differential expression analysis pipeline. To this end, the significant genes were defined as those with an FDR-adjusted *P* value < 0.05 using empirical Bayes F-tests. Therefore, we obtain the lists of genes that are differentially expressed between different grouping factors.

Gene set enrichment analyses

We performed the enrichment analysis using pathways in the Gene Ontology and REACTOME Database (MSigDB v2023.1.Hs, C2:CP:REACTOME, C5:GO:BP) *(99)* . The analyses were implemented using the R package ClusterProfiler *(101)*.The enriched pathways were defined as those with an FDR-adjusted *P* value < 0.05.

Identifying similarity between bulk RNA-Seq data with single-cell RNA-Seq data of microglia
To cross-validate the identification of our microglia samples on a transcriptomic level, we compared them with a publicly available single-cell RNA-Seq data set that comprises eight cell types from adult human brain samples, including microglia cells *(45)*. Briefly, we first identified the top 10 marker genes of each cell type following the standard *Seurat* workflow *(102)* . We then calculated the median expression level of these marker genes in each cell type. Finally, we performed the Pearson correlation tests between the median expression level of cell-type-specific marker of the eight cell types and their expression levels in each hiPSC-derived microglial sample.

The source code for data processing and analysis for this study has been deposited on Zenodo: https://zenodo.org/doi/10.5281/zenodo.12773329

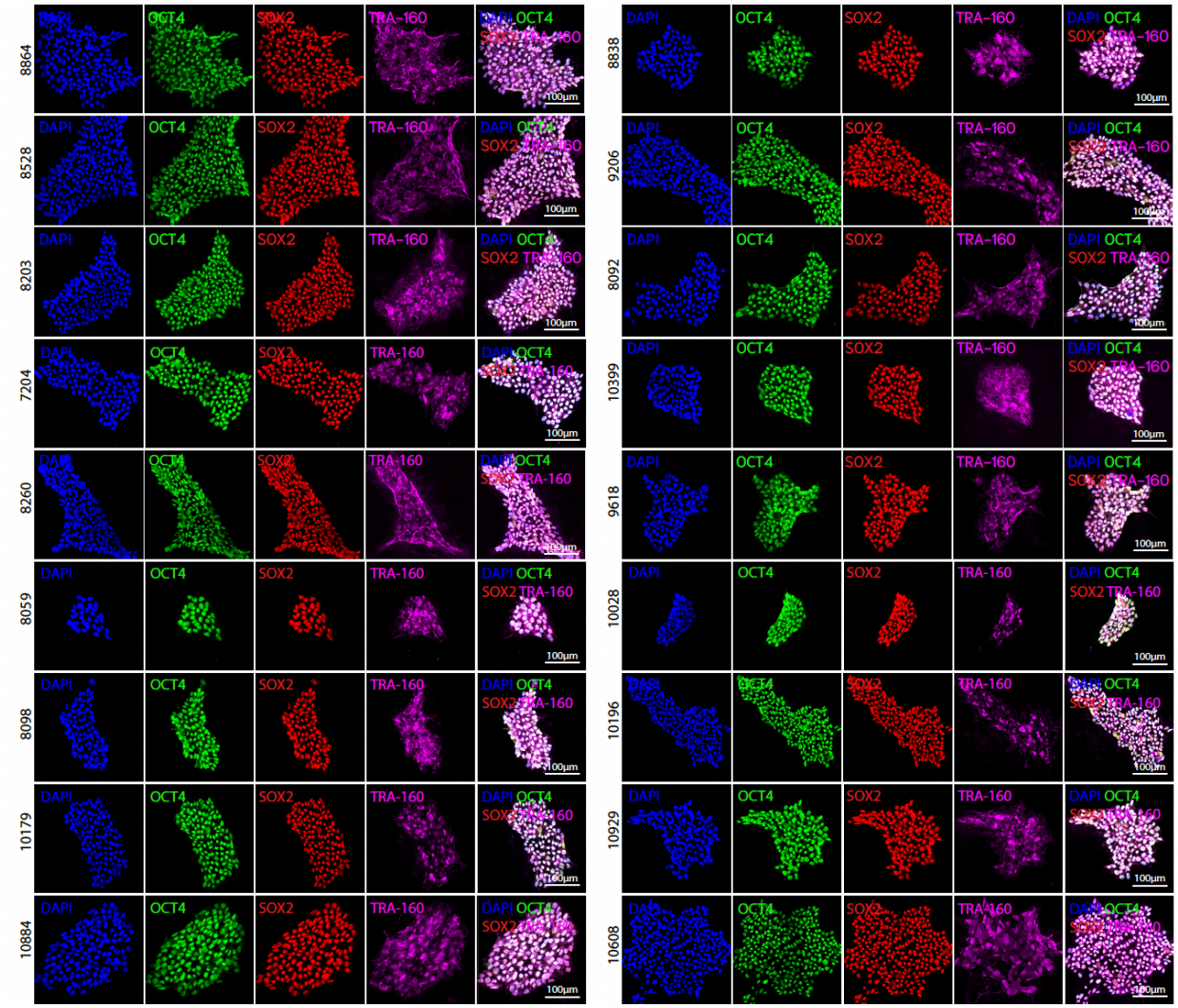

Fig. S1. Pluripotent markers of iPSC lines

All 18 lines were stained positive for pluripotent stem cell markers (OCT4, SOX2, TRA-1-60).

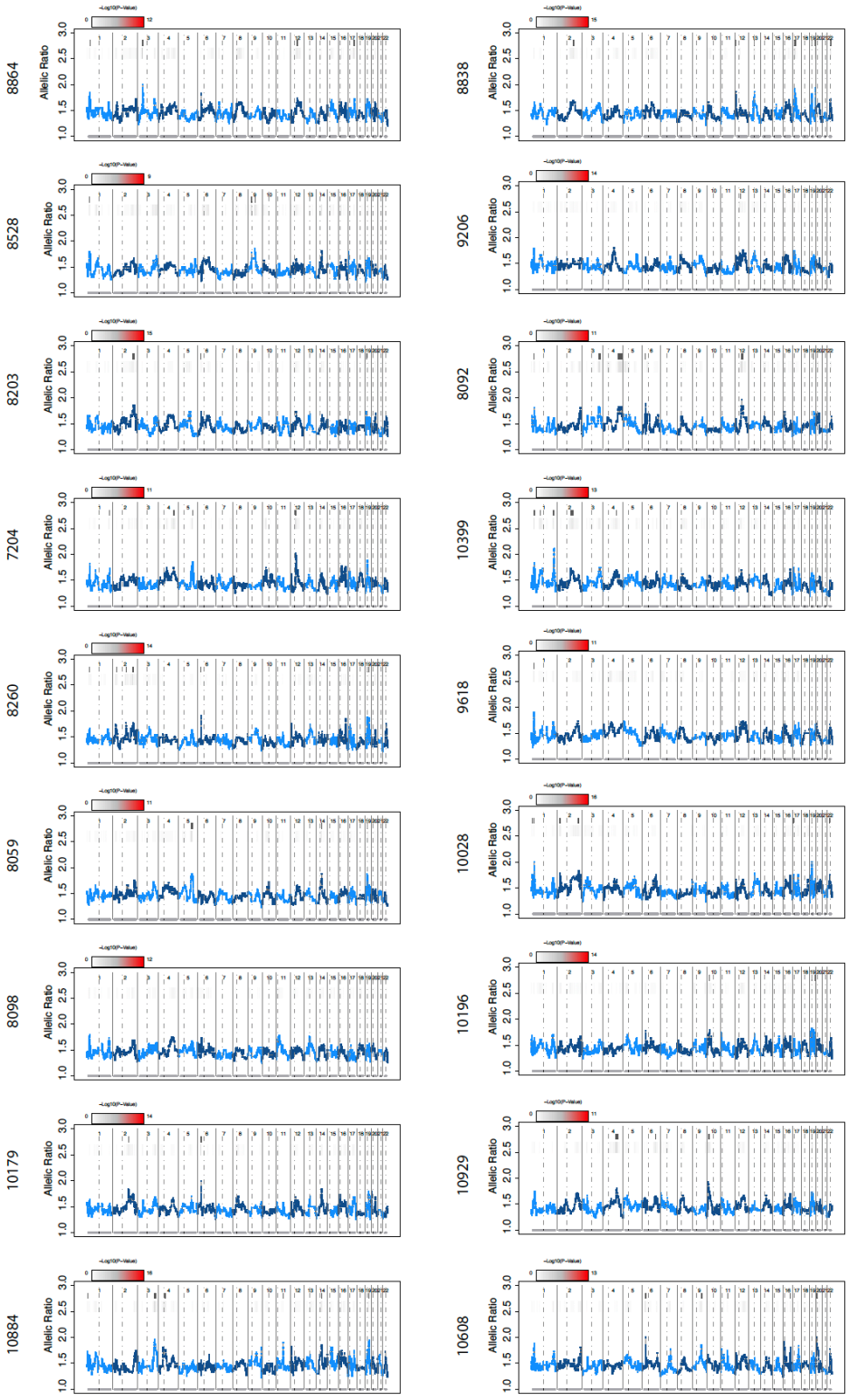

Fig. S2. eSNP-Karyotyping analysis of iPSC

The e-Karyotyping allelic ratio analysis for all 18 lines is represented by moving average plots of RNA-seq intensities for identified SNPs along the chromosomes. No significant instances of chromosome aneuploidy were observed in any of the iPSC lines. The color bars indicate the -$\log_{10}$ values of the FDR-corrected p-values.

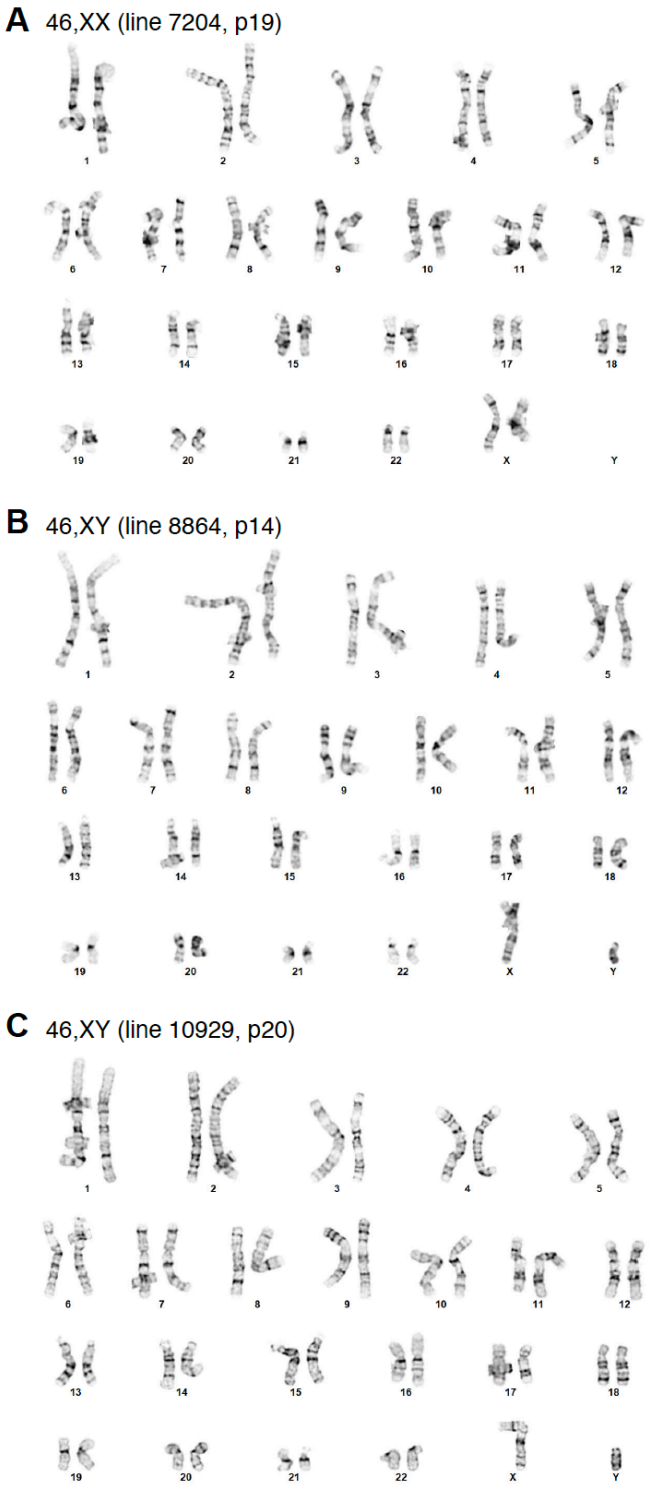

Fig. S3. G-band Karyotyping Analysis of iPSC
The G-band karyotyping analysis of three iPSC lines (A, B, and C) is shown. All three lines exhibit an apparently normal male karyotype, with representative karyotyped images.

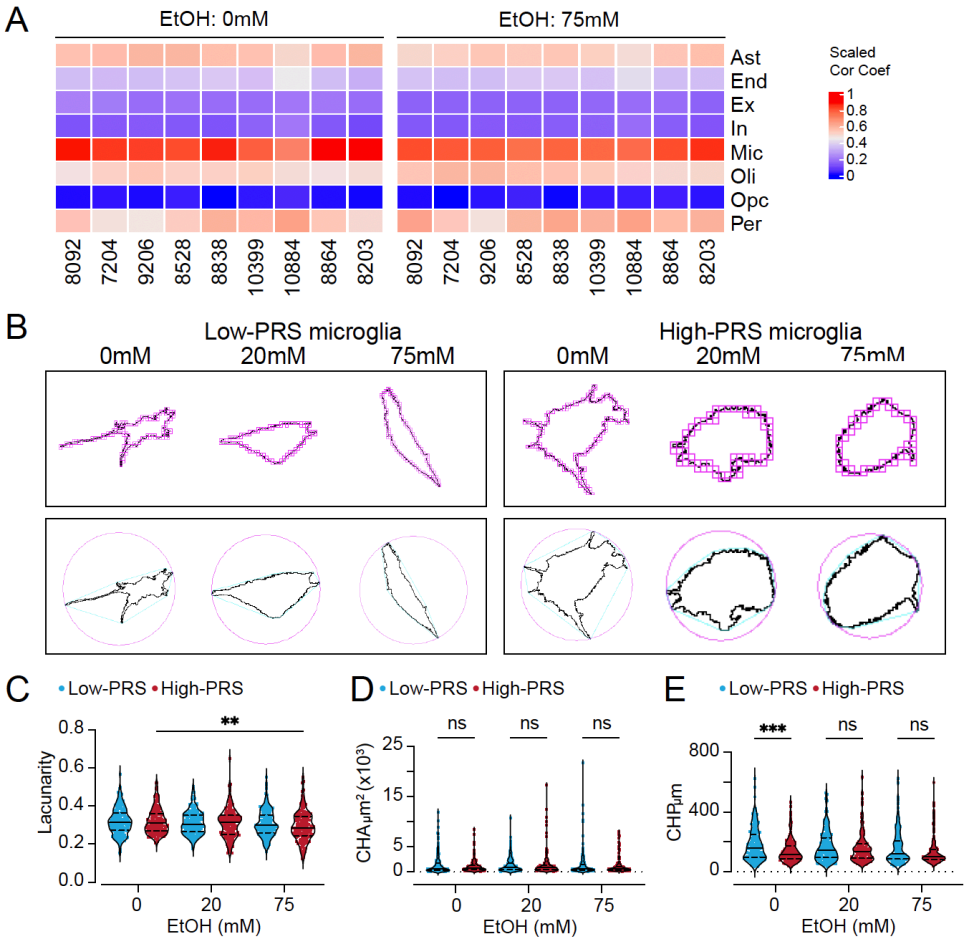

Fig. S4. Characterization of iPSC derived PMPs and microglia

(A) The correlation coefficient between the median expression levels of cell-type-specific genes in each cell type of scRNA-Seq data (rows) and their expression levels in each iPSC-derived microglial sample (columns, 5 low-PRS lines, 4 high-PRS lines). Ast: astrocytes; End: endothelial cells; Ex: excitatory neurons; In: inhibitory neurons, Mic: microglia; Oli: oligodendrocytes; Opc: oligodendrocyte precursor cells; Per: pericytes. **(B)** Upper: illustrating the box-counting method used for fractal dimension and lacunarity calculations. Lower: the associated convex hull (blue) and enclosing circle (pink) for corresponding outline shapes are used to calculate lacunarity, span ratio, and. (C-E) Morphological analysis of microglia binary outlines using FracLac ImageJ. n = 177 cells/high-PRS, 211 cells/low-PRS for 0 mM; n = 188 cells/high-PRS, 214 cells/low-PRS for 20 mM; n = 164 cells/high-PRS, 219 cells/low-PRS for 75 mM. * < 0.05, ** < 0.01, *** < 0.001. Data are presented as medium ± quartiles.

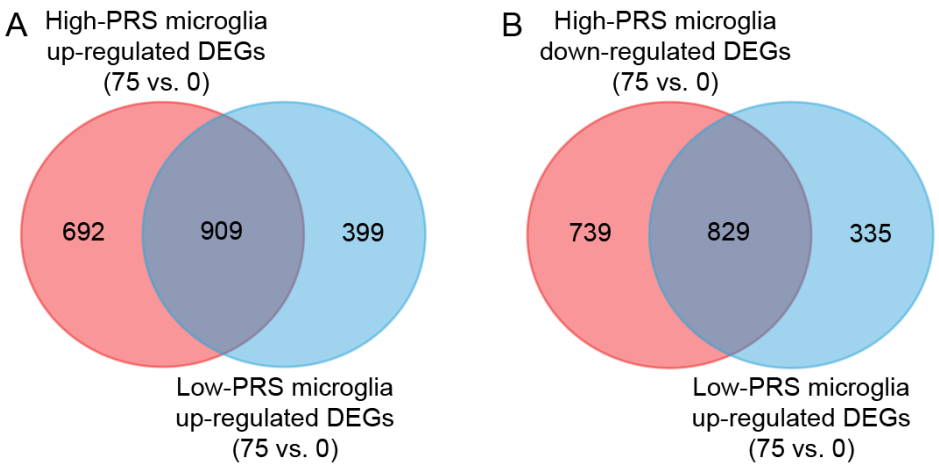

Fig. S5. Overlapping DEGs between high-PRS and low-PRS microglial cells

(A) Venn plot illustrating the overlap of upregulated DEGs between high-PRS and low-PRS microglial cells. **(B)** Venn plot illustrating the overlap of downregulated DEGs between high-PRS and low-PRS microglial cells.

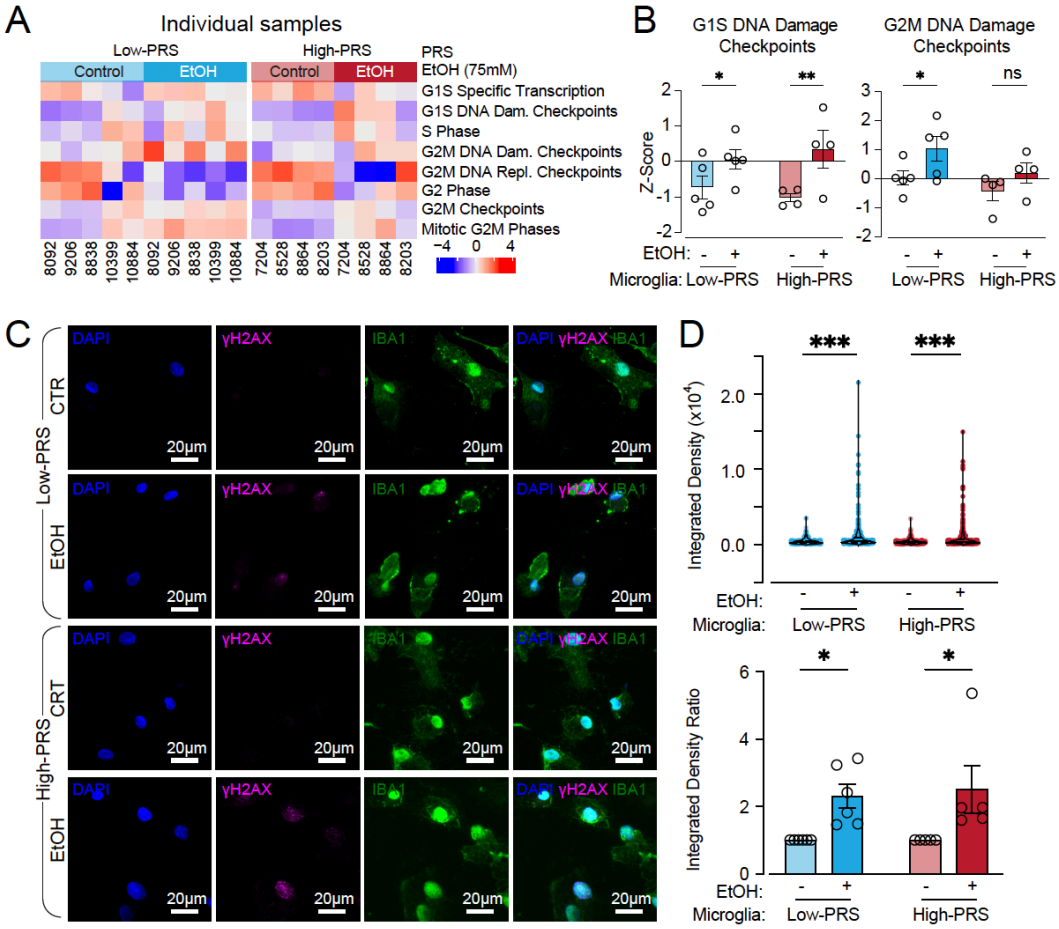

Fig. S6. DNA damage in high-PRS vs. low-PRS human microglia after ethanol exposure

(A) Heatmap illustration of the GSEA terms related to the cell cycle in both high-PRS (red, n = 4) and low-PRS (blue, n = 5) microglia, both before and after ethanol exposure. **(B)** Box plots illustrating the differential expression of GSEA terms related to the cell cycle in microglia from both high-PRS (red, n = 4) and low-PRS (blue, n =5) lines before and after ethanol treatment. low-PRS/high-PRS lines = 6/5. * < 0.05, ** < 0.01. Data are presented as mean ± SEM. **(C)** Representative images of γ-H2AX$^+$ and IBA1$^+$ microglia derived from PRS lines following treatment with ethanol (0 mM and 75 mM). **(D)** Upper: the quantification of γ-H2AX$^+$ fluorescence integrated density. n = 357 cells/5 high-PRS lines and 421 cells/6 low-PRS lines for 0 mM; n = 392 cells/5 high-PRS lines, 447 cells/6 low-PRS lines for 75 mM; ** < 0.01, *** < 0.001. Data are presented as mean ± SEM. Lower: the quantification of γ-H2AX$^+$ corrected fluorescence integrated density normalized to each control (0 mM) replicate. ** < 0.01, *** < 0.001. Data are presented as mean ± SEM.

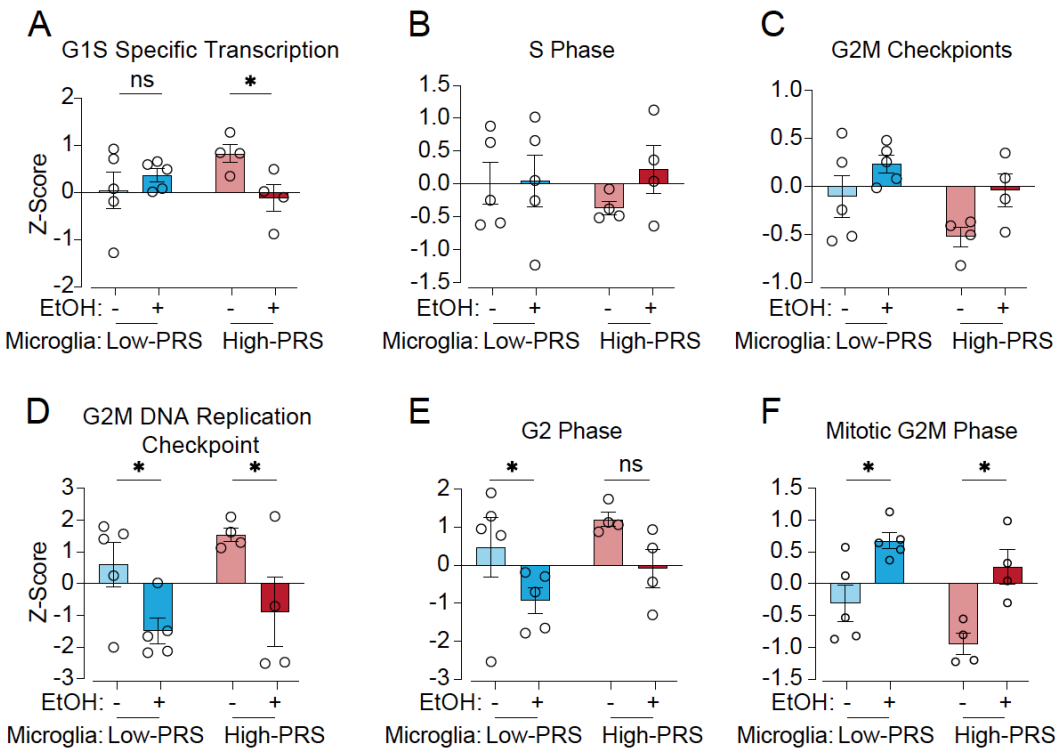

Fig. S7. Expression of GSEA terms related to the cell cycle in high-PRS and low-PRS microglial cells after ethanol exposure

(A-F) Box plots illustrating the differential expression of GSEA terms related to the cell cycle in microglial cells from both high-PRS (red, n=4 lines) and low-PRS (blue, n=5 lines) lines before and after Ethanol treatment. * < 0.05, ** < 0.01. Data are presented as mean ± SEM.

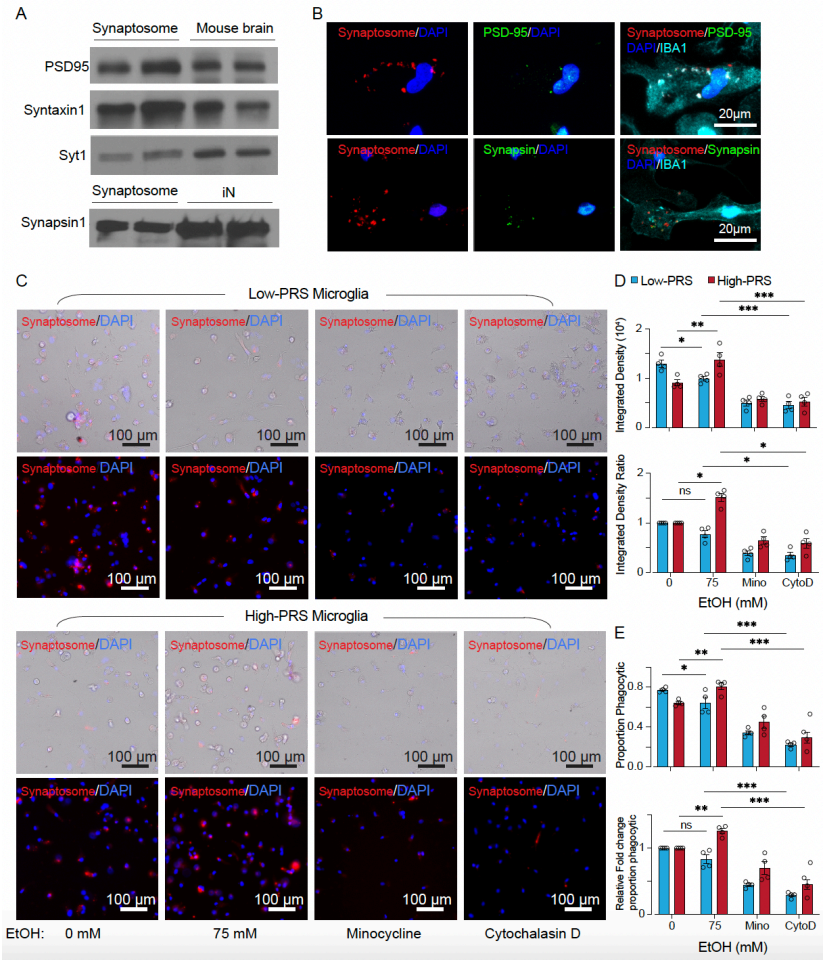

Fig. S8. Enhanced phagocytic ability of synaptosomes in high-PRS iPSC-derived microglia in response to ethanol

(A) Western blot analysis of synaptosomes extracted from iPSC-derived induced neurons**. (B)** Representative images of synaptosomes in IBA1^{+} microglia derived from high-PRS (line 8864). **(C)** Representative live-cell imaging of iPSC-derived microglia from low-PRS (line 10028) and high-PRS (line 8059) engaged in the phagocytosis of synaptosome. The upper images are overlapped with bright-field microscopy for reference. (D) Quantification of the fluorescence-integrated density of synaptosomes labeled with pHrodo™ Red dye: the upper panel shows the fluorescence-integrated density between high-PRS and low-PRS microglial cells, while the lower panel shows the corrected fluorescence-integrated density normalized to each control (0 mM). Low-PRS/high-PRS lines = 4/4, ** < 0.01, *** < 0.001. Data are presented as mean ± SEM. (E) Quantification of the proportion of microglia with synaptosomes labeled with pHrodo™ Red dye: the upper panel shows the proportion of microglia with beads, while the lower panel displays the corrected proportion, which has been normalized to each control (0 mM) replicate. Low-PRS/high-PRS lines = 4/4, ** < 0.01, *** < 0.001. Data are presented as mean ± SEM.

Table S1. Characteristics of individuals enrolled for iPSC generation and assays performed.

	Gender	Age	ID	PRS %ile	AUD	Bulk seq	Morphology & ICC	Phagocytosis assay	iN & Microglia Co-culture
High-PRS	male	38	8864	97.60	Yes	Yes	Yes	Yes	No
High-PRS	male	38	8528	97.70	Yes	Yes	Yes	Yes	No
High-PRS	male	38	8203	98.70	Yes	Yes	Yes	Yes	Yes
High-PRS	female	31	7204	98.80	Yes	Yes	Yes	Yes	Yes
High-PRS	female	39	8260	99.40	Yes	No	Yes	Yes	Yes
High-PRS	male	56	8059	95.56	Yes	No	No	Yes	Yes
High-PRS	female	28	8098	99.76	Yes	No	No	Yes	Yes
High-PRS	male	32	10179	75.50	Yes	No	No	Yes	Yes
Low-PRS	male	27	10884	1.40	No	Yes	Yes	Yes	No
Low-PRS	male	29	8838	2.80	No	Yes	Yes	Yes	No
Low-PRS	female	22	9206	0.90	No	Yes	Yes	Yes	No
Low-PRS	female	33	8092	5.10	No	Yes	Yes	Yes	Yes
Low-PRS	female	38	10399	0.89	No	Yes	Yes	Yes	Yes
Low-PRS	male	27	9618	0.40	No	No	Yes	Yes	Yes
Low-PRS	male	26	10028	13.09	No	No	No	Yes	Yes
Low-PRS	female	22	10196	4.24	No	No	No	Yes	Yes
Low-PRS	male	27	10929	1.44	No	No	No	Yes	Yes
Low-PRS	female	30	10608	9.96	No	No	No	Yes	Yes

Note: PRS: Polygenic risk scores; ICC: Immunological cytochemistry; Age: Subject age at time of lymphocyte collection.

Table S2. Gene expression count of ADH and ALDH genes in Bulk sequence from iPSC-derived microglia

Gene ID	Gene name	8092		7204		9206		8528		8838		10399		10884		8864		8203	
		0mM	75mM	0mM	75mM	0mM	75mM	0mM	75mM	0mM	75mM	0mM	75mM	0mM	75mM	0mM	75mM	0mM	75mM
ENSG00000187758	ADH1A	0	0	0	0	0	0	4	6	0	0	0	0	0	0	0	0	0	0
ENSG00000197894	ADH5	1618	1859	2084	1890	1612	1645	1572	1540	1579	1584	1522	1946	1686	1329	1461	1443	1424	1150
ENSG00000147576	ADHFE1	15	44	29	25	21	23	8	23	20	29	27	28	18	19	19	24	27	8
ENSG00000161618	ALDH16A1	1148	950	3112	1838	1760	1424	1812	1486	1088	1039	1929	1870	2189	1803	1613	1526	1754	1487
ENSG00000059573	ALDH18A1	159	140	177	188	131	142	197	185	180	159	190	283	168	253	200	210	197	149
ENSG00000165092	ALDH1A1	3	1	43	15	79	19	224	69	71	50	308	126	445	244	330	172	47	22
ENSG00000128918	ALDH1A2	7704	1993	8015	2556	3436	1006	10190	2009	2913	723	3997	2062	694	224	3563	1903	9678	4732
ENSG00000137124	ALDH1B1	63	27	188	103	137	90	91	40	75	42	35	58	151	108	52	64	171	68
ENSG00000136010	ALDH1L2	74	93	91	161	51	67	86	129	119	113	66	90	173	315	123	111	48	73
ENSG00000111275	ALDH2	657	848	697	952	692	802	857	1016	930	977	1179	1683	837	810	904	1558	310	538
ENSG00000072210	ALDH3A2	634	620	903	848	826	804	770	701	827	685	771	985	740	660	867	828	679	515
ENSG00000006534	ALDH3B1	1688	1745	2464	1745	1561	1515	1711	1713	1602	1461	1714	1844	2117	1993	1756	1771	2037	1401
ENSG00000159423	ALDH4A1	318	273	639	435	581	387	520	407	360	347	392	327	523	381	427	415	330	295
ENSG00000112294	ALDH5A1	188	95	449	206	229	142	298	82	212	83	376	271	54	95	289	192	742	204
ENSG00000119711	ALDH6A1	201	226	359	384	307	243	298	309	300	279	475	444	465	366	202	182	348	279
ENSG00000164904	ALDH7A1	463	543	719	711	709	678	513	737	623	586	593	807	623	708	611	770	489	521
ENSG00000143149	ALDH9A1	1599	1478	2154	1620	1820	1711	1849	1518	1437	1341	2162	2219	1703	1510	1432	1401	1657	1354
ENSG00000180011	ZADH2	993	855	1671	1392	1374	1249	1345	1158	1063	979	1343	1571	709	601	1149	992	1326	816

Table S3. General information of sequencing samples

sample	library	raw reads	raw bases	clean reads	clean bases	error rate	Q20	Q30	GC_pct
Low-PRS group									
8092 (0mM)	CRAS230023998-1r	42818486	6.42G	41406848	6.21G	0.02	97.99	94.45	52.2
8092 (75mM)	CRAS230024000-1r	42539472	6.38G	41198130	6.18G	0.02	98.06	94.54	52.51
8838 (0mM)	CRAS230024010-1r	45456668	6.82G	44053674	6.61G	0.02	98.11	94.67	52.46
8838 (75mM)	CRAS230024012-1r	43116898	6.47G	41864472	6.28G	0.02	97.97	94.35	53.01
10399 (0mM)	CRAS230024013-1r	48919870	7.34G	47371032	7.11G	0.02	98.06	94.53	52.5
10399 (75mM)	CRRA230024015-1a	64576460	9.69G	63074980	9.46G	0.03	97.56	93.78	54.05
10884 (0mM)	CRRA230024016-1a	51922120	7.79G	50675938	7.6G	0.03	97.7	93.91	53.13
10884 (75mM)	CRRA230024018-1a	46247992	6.94G	45096246	6.76G	0.03	97.59	93.65	53.62
9206 (0mM)	CRAS230024004-1r	46855900	7.03G	45152358	6.77G	0.02	98.13	94.75	52.59
9206 (75mM)	CRAS230024006-1r	45254386	6.79G	43866134	6.58G	0.02	98.08	94.6	52.92
High-PRS group									
8528 (0mM)	CRAS230024007-1r	50713000	7.61G	49252646	7.39G	0.02	97.93	94.28	52.68
8528 (75mM)	CRAS230024009-1r	50651220	7.6G	48944528	7.34G	0.03	97.92	94.27	53.17
8864 (0mM)	CRRA230024019-1a	44768638	6.72G	43974814	6.6G	0.03	97.57	93.6	52.9
8864 (75mM)	CRRA230024021-1a	51643684	7.75G	50863276	7.63G	0.03	97.74	93.94	53.24
8203 (0mM)	CRRA230024022-1a	49572568	7.44G	48741338	7.31G	0.03	97.67	93.9	52.86
8203 (75mM)	CRRA230024024-1a	42315166	6.35G	41459172	6.22G	0.03	97.78	94.06	53
7204 (0mM)	CRAS230024001-1r	65632920	9.84G	61952374	9.29G	0.02	98.07	94.45	54.21
7204 (75mM)	CRAS230024003-1r	54570298	8.19G	52910082	7.94G	0.03	97.9	94.16	52.61

REFERENCES AND NOTES

1. A. F. Carvalho, M. Heilig, A. Perez, C. Probst, J. Rehm, Alcohol use disorders. *Lancet* **394**, 781–792 (2019).

2. B. Verhulst, M. C. Neale, K. S. Kendler, The heritability of alcohol use disorders: A meta-analysis of twin and adoption studies. *Psychol. Med.* **45**, 1061–1072 (2015).

3. G. R. B. Saunders, X. Wang, F. Chen, S. K. Jang, M. Liu, C. Wang, S. Gao, Y. Jiang, C. Khunsriraksakul, J. M. Otto, C. Addison, M. Akiyama, C. M. Albert, F. Aliev, A. Alonso, D. K. Arnett, A. E. Ashley-Koch, A. A. Ashrani, K. C. Barnes, R. G. Barr, T. M. Bartz, D. M. Becker, L. F. Bielak, E. J. Benjamin, J. C. Bis, G. Bjornsdottir, J. Blangero, E. R. Bleecker, J. D. Boardman, E. Boerwinkle, D. I. Boomsma, M. P. Boorgula, D. W. Bowden, J. A. Brody, B. E. Cade, D. I. Chasman, S. Chavan, Y. I. Chen, Z. Chen, I. Cheng, M. H. Cho, H. Choquet, J. W. Cole, M. C. Cornelis, F. Cucca, J. E. Curran, M. de Andrade, D. M. Dick, A. R. Docherty, R. Duggirala, C. B. Eaton, M. A. Ehringer, T. Esko, J. D. Faul, L. Fernandes Silva, E. Fiorillo, M. Fornage, B. I. Freedman, M. E. Gabrielsen, M. E. Garrett, S. A. Gharib, C. Gieger, N. Gillespie, D. C. Glahn, S. D. Gordon, C. C. Gu, D. Gu, D. F. Gudbjartsson, X. Guo, J. Haessler, M. E. Hall, T. Haller, K. M. Harris, J. He, P. Herd, J. K. Hewitt, I. Hickie, B. Hidalgo, J. E. Hokanson, C. Hopfer, J. Hottenga, L. Hou, H. Huang, Y. J. Hung, D. J. Hunter, K. Hveem, S. J. Hwang, C. M. Hwu, W. Iacono, M. R. Irvin, Y. H. Jee, E. O. Johnson, Y. Y. Joo, E. Jorgenson, A. E. Justice, Y. Kamatani, R. C. Kaplan, J. Kaprio, S. L. R. Kardia, M. C. Keller, T. N. Kelly, C. Kooperberg, T. Korhonen, P. Kraft, K. Krauter, J. Kuusisto, M. Laakso, J. Lasky-Su, W. J. Lee, J. J. Lee, D. Levy, L. Li, K. Li, Y. Li, K. Lin, P. A. Lind, C. Liu, D. M. Lloyd-Jones, S. M. Lutz, J. Ma, R. Mägi, A. Manichaikul, N. G. Martin, R. Mathur, N. Matoba, P. F. McArdle, M. McGue, M. B. McQueen, S. E. Medland, A. Metspalu, D. A. Meyers, I. Y. Millwood, B. D. Mitchell, K. L. Mohlke, M. Moll, M. E. Montasser, A. C. Morrison, A. Mulas, J. B. Nielsen, K. E. North, E. C. Oelsner, Y. Okada, V. Orrù, N. D. Palmer, T. Palviainen, A. Pandit, S. L. Park, U. Peters, A. Peters, P. A. Peyser, T. J. C. Polderman, N. Rafaels, S. Redline, R. M. Reed, A. P. Reiner, J. P. Rice, S. S. Rich, N. E. Richmond, C. Roan, J. I. Rotter, M. N. Rueschman, V. Runarsdottir, N. L. Saccone, D. A. Schwartz, A. H. Shadyab, J. Shi, S. S. Shringarpure, K. Sicinski, A. H. Skogholt, J. A. Smith, N. L. Smith, N. Sotoodehnia, M. C. Stallings, H.

Stefansson, K. Stefansson, J. A. Stitzel, X. Sun, M. Syed, R. Tal-Singer, A. E. Taylor, K. D. Taylor, M. J. Telen, K. K. Thai, H. Tiwari, C. Turman, T. Tyrfingsson, T. L. Wall, R. G. Walters, D. R. Weir, S. T. Weiss, W. B. White, J. B. Whitfield, K. L. Wiggins, G. Willemsen, C. J. Willer, B. S. Winsvold, H. Xu, L. R. Yanek, J. Yin, K. L. Young, K. A. Young, B. Yu, W. Zhao, W. Zhou, S. Zöllner, L. Zuccolo, C. Batini, A. W. Bergen, L. J. Bierut, S. P. David, S. A. Gagliano Taliun, D. B. Hancock, B. Jiang, M. R. Munafò, T. E. Thorgeirsson, D. J. Liu, S. Vrieze, Genetic diversity fuels gene discovery for tobacco and alcohol use. *Nature* **612**, 720–724 (2022).

4. J. Su, S. I. Kuo, F. Aliev, J. A. Rabinowitz, B. Jamil, G. Chan, H. J. Edenberg, M. Francis, V. Hesselbrock, C. Kamarajan, S. Kinreich, J. Kramer, D. Lai, V. McCutcheon, J. Meyers, A. Pandey, G. Pandey, M. H. Plawecki, M. Schuckit, J. Tischfield, D. M. Dick, Alcohol use polygenic risk score, social support, and alcohol use among European American and African American adults, in *Development and Psychopathology* (Cambridge Univ. Press, (2023), pp. 1–13.

5. J. D. Deak, E. C. Johnson, Genetics of substance use disorders: A review. *Psychol. Med.* **51**, 2189–2200 (2021).

6. H. R. Kranzler, H. Zhou, R. L. Kember, R. Vickers Smith, A. C. Justice, S. Damrauer, P. S. Tsao, D. Klarin, A. Baras, J. Reid, J. Overton, D. J. Rader, Z. Cheng, J. P. Tate, W. C. Becker, J. Concato, K. Xu, R. Polimanti, H. Zhao, J. Gelernter, Genome-wide association study of alcohol consumption and use disorder in 274,424 individuals from multiple populations. *Nat. Commun.* **10**, 1499 (2019).

7. A. B. Hart, H. R. Kranzler, Alcohol dependence genetics: lessons learned from genome-wide association studies (GWAS) and post-GWAS analyses. *Alcohol Clin. Exp. Res.* **39**, 1312–1327 (2015).

8. N. R. Wray, S. H. Lee, D. Mehta, A. A. Vinkhuyzen, F. Dudbridge, C. M. Middeldorp, Research review: Polygenic methods and their application to psychiatric traits. *J. Child. Psychol. Psychiatry* **55**, 1068–1087 (2014).

9. G. Ni, J. Zeng, J. A. Revez, Y. Wang, Z. Zheng, T. Ge, R. Restuadi, J. Kiewa, D. R. Nyholt, J. R. I. Coleman, J. W. Smoller, J. Yang, P. M. Visscher, N. R. Wray, A comparison of ten polygenic score methods for psychiatric disorders applied across multiple cohorts. *Biol. Psychiatry* **90**, 611–620 (2021).

10. D. Lai, E. C. Johnson, S. Colbert, G. Pandey, G. Chan, L. Bauer, M. W. Francis, V. Hesselbrock, C. Kamarajan, J. Kramer, W. Kuang, S. Kuo, S. Kuperman, Y. Liu, V. McCutcheon, Z. Pang, M. H. Plawecki, M. Schuckit, J. Tischfield, L. Wetherill, Y. Zang, H. J. Edenberg, B. Porjesz, A. Agrawal, T. Foroud, Evaluating risk for alcohol use disorder: Polygenic risk scores and family history. *Alcohol Clin. Exp. Res.* **46**, 374–383 (2022).

11. J. E. Savage, J. E. Salvatore, F. Aliev, A. C. Edwards, M. Hickman, K. S. Kendler, J. Macleod, A. Latvala, A. Loukola, J. Kaprio, R. J. Rose, G. Chan, V. Hesselbrock, B. T. Webb, A. Adkins, T. B. Bigdeli, B. P. Riley, D. M. Dick, Polygenic risk score prediction of alcohol dependence symptoms across population-based and clinically ascertained samples. *Alcohol Clin. Exp. Res.* **42**, 520–530 (2018).

12. P. B. Barr, A. Ksinan, J. Su, E. C. Johnson, J. L. Meyers, L. Wetherill, A. Latvala, F. Aliev, G. Chan, S. Kuperman, J. Nurnberger, C. Kamarajan, A. Anokhin, A. Agrawal, R. J. Rose, H. J. Edenberg, M. Schuckit, J. Kaprio, D. M. Dick, Using polygenic scores for identifying individuals at increased risk of substance use disorders in clinical and population samples. *Transl. Psychiatry* **10**, 196 (2020).

13. E. K. Erickson, E. K. Grantham, A. S. Warden, R. A. Harris, Neuroimmune signaling in alcohol use disorder. *Pharmacol. Biochem. Behav.* **177**, 34–60 (2019).

14. M. Kapoor, J. C. Wang, S. P. Farris, Y. Liu, J. McClintick, I. Gupta, J. L. Meyers, S. Bertelsen, M. Chao, J. Nurnberger, J. Tischfield, O. Harari, L. Zeran, V. Hesselbrock, L. Bauer, T. Raj, B. Porjesz, A. Agrawal, T. Foroud, H. J. Edenberg, R. D. Mayfield, A. Goate, Analysis of whole genome-transcriptomic organization in brain to identify genes associated with alcoholism. *Transl. Psychiatry* **9**, 89 (2019).

15. L. De Filippis, A. Halikere, H. McGowan, J. C. Moore, J. A. Tischfield, R. P. Hart, Z. P. Pang, Ethanol-mediated activation of the NLRP3 inflammasome in iPS cells and iPS cells-derived neural progenitor cells. *Mol. Brain* **9**, 51 (2016).

16. V. H. Perry, A revised view of the central nervous system microenvironment and major histocompatibility complex class II antigen presentation. *J. Neuroimmunol.* **90**, 113–121 (1998).

17. D. Gosselin, D. Skola, N. G. Coufal, I. R. Holtman, J. C. M. Schlachetzki, E. Sajti, B. N. Jaeger, C. O'Connor, C. Fitzpatrick, M. P. Pasillas, M. Pena, A. Adair, D. D. Gonda, M. L. Levy, R. M. Ransohoff, F. H. Gage, C. K. Glass, An environment-dependent transcriptional network specifies human microglia identity. *Science* **356**, eaal3222 (2017).

18. T. R. Hammond, C. Dufort, L. Dissing-Olesen, S. Giera, A. Young, A. Wysoker, A. J. Walker, F. Gergits, M. Segel, J. Nemesh, S. E. Marsh, A. Saunders, E. Macosko, F. Ginhoux, J. Chen, R. J. M. Franklin, X. Piao, S. A. McCarroll, B. Stevens, Single-cell RNA sequencing of microglia throughout the mouse lifespan and in the injured brain reveals complex cell-state changes. *Immunity* **50**, 253–271.e6 (2019).

19. T. Matsudaira, M. Prinz, Life and death of microglia: Mechanisms governing microglial states and fates. *Immunol. Lett.* **245**, 51–60 (2022).

20. Y. Liu, X. Shen, Y. Zhang, X. Zheng, C. Cepeda, Y. Wang, S. Duan, X. Tong, Interactions of glial cells with neuronal synapses, from astrocytes to microglia and oligodendrocyte lineage cells. *Glia* **71**, 1383–1401 (2023).

21. D. P. Schafer, E. K. Lehrman, A. G. Kautzman, R. Koyama, A. R. Mardinly, R. Yamasaki, R. M. Ransohoff, M. E. Greenberg, B. A. Barres, B. Stevens, Microglia sculpt postnatal neural circuits in an activity and complement-dependent manner. *Neuron* **74**, 691–705 (2012).

22. S. A. Marshall, C. R. Geil, K. Nixon, Prior binge ethanol exposure potentiates the microglial response in a model of alcohol-induced neurodegeneration. *Brain Sci.* **6**, 16 (2016).

23. S. A. Marshall, J. A. McClain, M. L. Kelso, D. M. Hopkins, J. R. Pauly, K. Nixon, Microglial activation is not equivalent to neuroinflammation in alcohol-induced neurodegeneration: The importance of microglia phenotype. *Neurobiol. Dis.* **54**, 239–251 (2013).

24. S. Mukherjee, M. A. Cabrera, N. I. Boyadjieva, G. Berger, B. Rousseau, D. K. Sarkar, Alcohol increases exosome release from microglia to promote complement C1q-induced cellular death of proopiomelanocortin neurons in the hypothalamus in a rat model of fetal alcohol spectrum disorders. *J. Neurosci.* **40**, 7965–7979 (2020).

25. L. G. Chastain, D. K. Sarkar, Role of microglia in regulation of ethanol neurotoxic action. *Int. Rev. Neurobiol.* **118**, 81–103 (2014).

26. T. J. Walter, F. T. Crews, Microglial depletion alters the brain neuroimmune response to acute binge ethanol withdrawal. *J. Neuroinflammation* **14**, 86 (2017).

27. A. S. Warden, S. A. Wolfe, S. Khom, F. P. Varodayan, R. R. Patel, M. Q. Steinman, M. Bajo, S. E. Montgomery, R. Vlkolinsky, T. Nadav, I. Polis, A. J. Roberts, R. D. Mayfield, R. A. Harris, M. Roberto, Microglia control escalation of drinking in alcohol-dependent mice: Genomic and synaptic drivers. *Biol. Psychiatry* **88**, 910–921 (2020).

28. L. Lan, H. Wang, X. Zhang, Q. Shen, X. Li, L. He, X. Rong, J. Peng, J. Mo, Y. Peng, Chronic exposure of alcohol triggers microglia-mediated synaptic elimination inducing cognitive impairment. *Exp. Neurol.* **353**, 114061 (2022).

29. T. F. Galatro, I. R. Holtman, A. M. Lerario, I. D. Vainchtein, N. Brouwer, P. R. Sola, M. M. Veras, T. F. Pereira, R. E. P. Leite, T. Möller, P. D. Wes, M. C. Sogayar, J. D. Laman, W. den Dunnen, C. A. Pasqualucci, S. M. Oba-Shinjo, E. Boddeke, S. K. N. Marie, B. J. L. Eggen, Transcriptomic analysis of purified human cortical microglia reveals age-associated changes. *Nat. Neurosci.* **20**, 1162–1171 (2017).

30. R. Xu, X. Li, A. J. Boreland, A. Posyton, K. Kwan, R. P. Hart, P. Jiang, Human iPSC-derived mature microglia retain their identity and functionally integrate in the chimeric mouse brain. *Nat. Commun.* **11**, 1577 (2020).

31. E. M. Abud, R. N. Ramirez, E. S. Martinez, L. M. Healy, C. H. H. Nguyen, S. A. Newman, A. V. Yeromin, V. M. Scarfone, S. E. Marsh, C. Fimbres, C. A. Caraway, G. M. Fote, A. M. Madany, A. Agrawal, R. Kayed, K. H. Gylys, M. D. Cahalan, B. J. Cummings, J. P. Antel, A. Mortazavi, M. J. Carson, W. W. Poon, M. Blurton-Jones, iPSC-derived human microglia-like cells to study neurological diseases. *Neuron* **94**, 278–293.e9 (2017).

32. R. Xu, A. J. Boreland, X. Li, C. Erickson, M. Jin, C. Atkins, Z. Pang, B. P. Daniels, P. Jiang, Developing human pluripotent stem cell-based cerebral organoids with a controllable microglia ratio for modeling brain development and pathology. *Stem Cell Rep.* **16**, 1923–1937 (2020).

33. S. R. Guttikonda, L. Sikkema, J. Tchieu, N. Saurat, R. M. Walsh, O. Harschnitz, G. Ciceri, M. Sneeboer, L. Mazutis, M. Setty, P. Zumbo, D. Betel, L. D. de Witte, D. Pe'er, L. Studer, Fully defined human pluripotent stem cell-derived microglia and tri-culture system model C3 production in Alzheimer's disease. *Nat. Neurosci.* **24**, 343–354 (2021).

34. M. Jin, Z. Ma, P. Jiang, Generation of iPSC-based human-mouse microglial brain chimeras to study senescence of human microglia. *STAR Protoc.* **3**, 101847 (2022).

35. D. S. Svoboda, M. I. Barrasa, J. Shu, R. Rietjens, S. Zhang, M. Mitalipova, P. Berube, D. Fu, L. D. Shultz, G. W. Bell, R. Jaenisch, Human iPSC-derived microglia assume a primary microglia-like state after transplantation into the neonatal mouse brain. *Proc. Natl. Acad. Sci. U.S.A.* **116**, 25293–25303 (2019).

36. A. J. Boreland, A. C. Stillitano, H. C. Lin, Y. Abbo, R. P. Hart, P. Jiang, Z. P. Pang, A. B. Rabson, Dysregulated neuroimmune interactions and sustained type I interferon signaling after human immunodeficiency virus type 1 infection of human iPSC derived microglia and cerebral organoids. bioRxiv 563950 [Preprint] (2023).

37. M. J. Dolan, M. Therrien, S. Jereb, T. Kamath, V. Gazestani, T. Atkeson, S. E. Marsh, A. Goeva, N. M. Lojek, S. Murphy, C. M. White, J. Joung, B. Liu, F. Limone, K. Eggan, N. Hacohen, B. E. Bernstein, C. K. Glass, V. Leinonen, M. Blurton-Jones, F. Zhang, C. B. Epstein, E. Z. Macosko, B. Stevens, Exposure of iPSC-derived human microglia to brain substrates

enables the generation and manipulation of diverse transcriptional states in vitro. *Nat. Immunol.* **24**, 1382–1390 (2023).

38. J. F. Henriques, C. C. Portugal, T. Canedo, J. B. Relvas, T. Summavielle, R. Socodato, Microglia and alcohol meet at the crossroads: Microglia as critical modulators of alcohol neurotoxicity. *Toxicol. Lett.* **283**, 21–31 (2018).

39. E. K. Erickson, Y. A. Blednov, R. A. Harris, R. D. Mayfield, Glial gene networks associated with alcohol dependence. *Sci Rep* **9**, 10949 (2019).

40. J. He, F. T. Crews, Increased MCP-1 and microglia in various regions of the human alcoholic brain. *Exp. Neurol.* **210**, 349–358 (2008).

41. E. C. Johnson, J. E. Salvatore, D. Lai, A. K. Merikangas, J. I. Nurnberger, J. A. Tischfield, X. Xuei, C. Kamarajan, L. Wetherill, J. P. Rice, J. R. Kramer, S. Kuperman, T. Foroud, P. A. Slesinger, A. M. Goate, B. Porjesz, D. M. Dick, H. J. Edenberg, A. Agrawal, The collaborative study on the genetics of alcoholism: Genetics. *Genes Brain Behav.* **22**, e12856 (2023).

42. A. Agrawal, S. J. Brislin, K. K. Bucholz, D. Dick, R. P. Hart, E. C. Johnson, J. Meyers, J. Salvatore, P. Slesinger, C. Collaborators, L. Almasy, T. Foroud, A. Goate, V. Hesselbrock, J. Kramer, S. Kuperman, A. K. Merikangas, J. I. Nurnberger, J. Tischfield, H. J. Edenberg, B. Porjesz, The collaborative study on the genetics of alcoholism: Overview. *Genes Brain Behav.* **22**, e12864 (2023).

43. I. Gameiro-Ros, D. Popova, I. Prytkova, Z. P. Pang, Y. Liu, D. Dick, K. K. Bucholz, A. Agrawal, B. Porjesz, A. M. Goate, X. Xuei, C. Kamarajan, C. Collaborators, J. A. Tischfield, H. J. Edenberg, P. A. Slesinger, R. P. Hart, 5. Collaborative study on the genetics of alcoholism: Functional genomics. *Genes Brain Behav.* **22**, e12855 (2023).

44. U. Weissbein, M. Schachter, D. Egli, N. Benvenisty, Analysis of chromosomal aberrations and recombination by allelic bias in RNA-seq. *Nat. Commun.* **7**, 12144 (2016).

45. H. Mathys, Z. Peng, C. A. Boix, M. B. Victor, N. Leary, S. Babu, G. Abdelhady, X. Jiang, A. P. Ng, K. Ghafari, A. K. Kunisky, J. Mantero, K. Galani, V. N. Lohia, G. E. Fortier, Y. Lotfi, J.

Ivey, H. P. Brown, P. R. Patel, N. Chakraborty, J. I. Beaudway, E. J. Imhoff, C. F. Keeler, M. M. McChesney, H. H. Patel, S. P. Patel, M. T. Thai, D. A. Bennett, M. Kellis, L. H. Tsai, Single-cell atlas reveals correlates of high cognitive function, dementia, and resilience to Alzheimer's disease pathology. *Cell* **186**, 4365–4385.e27 (2023).

46. M. S. Scarnati, A. Halikere, Z. P. Pang, Using human stem cells as a model system to understand the neural mechanisms of alcohol use disorders: Current status and outlook. *Alcohol* **74**, 83–93 (2019).

47. J. Cornell, S. Salinas, H. Y. Huang, M. Zhou, Microglia regulation of synaptic plasticity and learning and memory. *Neural Regen. Res.* **17**, 705–716 (2022).

48. Q. Li, D. Liu, F. Pan, C. S. H. Ho, R. C. M. Ho, Ethanol exposure induces microglia activation and neuroinflammation through TLR4 activation and SENP6 modulation in the adolescent rat hippocampus. *Neural Plast.* **2019**, 1648736 (2019).

49. A. M. Jurga, M. Paleczna, K. Z. Kuter, Overview of general and discriminating markers of differential microglia phenotypes. *Front. Cell Neurosci.* **14**, 198 (2020).

50. M. Prinz, S. Jung, J. Priller, Microglia biology: One century of evolving concepts. *Cell* **179**, 292–311 (2019).

51. H. J. Edenberg, J. N. McClintick, alcohol dehydrogenases, aldehyde dehydrogenases, and alcohol use disorders: A critical review. *Alcohol Clin. Exp. Res.* **42**, 2281–2297 (2018).

52. M. E. Deerhake, M. L. Shinohara, Emerging roles of Dectin-1 in noninfectious settings and in the CNS. *Trends Immunol.* **42**, 891–903 (2021).

53. L. J. Mah, A. El-Osta, T. C. Karagiannis, γH2AX: A sensitive molecular marker of DNA damage and repair. *Leukemia* **24**, 679–686 (2010).

54. J. K. Sun, D. Wu, G. C. Wong, T. M. Lau, M. Yang, R. P. Hart, K. M. Kwan, H. Y. E. Chan, H. M. Chow, Chronic alcohol metabolism results in DNA repair infidelity and cell cycle-induced senescence in neurons. *Aging Cell* **22**, e13772 (2023).

55. S. Bang, C. R. Donnelly, X. Luo, M. Toro-Moreno, X. Tao, Z. Wang, S. Chandra, A. V. Bortsov, E. R. Derbyshire, R. R. Ji, Activation of GPR37 in macrophages confers protection against infection-induced sepsis and pain-like behaviour in mice. *Nat. Commun.* **12**, 1704 (2021).

56. E. Layman, J. M. Parrott, H. Y. Lee, Protocol for assessing phagocytosis activity in cultured primary murine microglia. *STAR Protoc.* **3**, 101881 (2022).

57. Y. Zhang, C. Pak, Y. Han, H. Ahlenius, Z. Zhang, S. Chanda, S. Marro, C. Patzke, C. Acuna, J. Covy, W. Xu, N. Yang, T. Danko, L. Chen, M. Wernig, T. C. Südhof, Rapid single-step induction of functional neurons from human pluripotent stem cells. *Neuron* **78**, 785–798 (2013).

58. D. Popova, I. Gameiro-Ros, M. M. Youssef, P. Zalamea, A. D. Morris, I. Prytkova, A. Jadali, K. Y. Kwan, C. Kamarajan, J. E. Salvatore, X. Xuei, D. B. Chorlian, B. Porjesz, S. Kuperman, D. M. Dick, A. Goate, H. J. Edenberg, J. A. Tischfield, Z. P. Pang, P. A. Slesinger, R. P. Hart, Alcohol reverses the effects of KCNJ6 (GIRK2) noncoding variants on excitability of human glutamatergic neurons. *Mol. Psychiatry* **28**, 746–758 (2023).

59. T. Vierbuchen, A. Ostermeier, Z. P. Pang, Y. Kokubu, T. C. Sudhof, M. Wernig, Direct conversion of fibroblasts to functional neurons by defined factors. *Nature* **463**, 1035–1041 (2010).

60. Z. P. Pang, N. Yang, T. Vierbuchen, A. Ostermeier, D. R. Fuentes, T. Q. Yang, A. Citri, V. Sebastiano, S. Marro, T. C. Südhof, M. Wernig, Induction of human neuronal cells by defined transcription factors. *Nature* **476**, 220–223 (2011).

61. L. J. Lawson, V. H. Perry, P. Dri, S. Gordon, Heterogeneity in the distribution and morphology of microglia in the normal adult mouse brain. *Neuroscience* **39**, 151–170 (1990).

62. J. A. Fantuzzo, V. R. Mirabella, A. H. Hamod, R. P. Hart, J. D. Zahn, Z. P. Pang, *Intellicount*: High-throughput quantification of fluorescent synaptic protein puncta by machine learning. *eNeuro* **4**, ENEURO.0219-17.2017 (2017).

63. D. H. Geschwind, J. Flint, Genetics and genomics of psychiatric disease. *Science* **349**, 1489–1494 (2015).

64. P. M. Visscher, N. R. Wray, Q. Zhang, P. Sklar, M. I. McCarthy, M. A. Brown, J. Yang, 10 Years of GWAS discovery: Biology, function, and translation. *Am. J. Hum. Genet.* **101**, 5–22 (2017).

65. D. Lvovs, O. O. Favorova, A. V. Favorov, A polygenic approach to the study of polygenic diseases. *Acta Naturae* **4**, 59–71 (2012).

66. A. Nimmerjahn, F. Kirchhoff, F. Helmchen, Resting microglial cells are highly dynamic surveillants of brain parenchyma in vivo. *Science* **308**, 1314–1318 (2005).

67. H. Kettenmann, U. K. Hanisch, M. Noda, A. Verkhratsky, Physiology of microglia. *Physiol. Rev.* **91**, 461–553 (2011).

68. M. Colonna, O. Butovsky, Microglia function in the central nervous system during health and neurodegeneration. *Annu. Rev. Immunol.* **35**, 441–468 (2017).

69. A. R. Mantegazza, J. G. Magalhaes, S. Amigorena, M. S. Marks, Presentation of phagocytosed antigens by MHC class I and II. *Traffic* **14**, 135–152 (2013).

70. V. Maneu, A. Yáñez, C. Murciano, A. Molina, M. L. Gil, D. Gozalbo, Dectin-1 mediates in vitro phagocytosis of Candida albicans yeast cells by retinal microglia. *FEMS Immunol. Med. Microbiol.* **63**, 148–150 (2011).

71. A. Pellon, A. Ramirez-Garcia, X. Guruceaga, A. Zabala, I. Buldain, A. Antoran, J. Anguita, A. Rementeria, C. Matute, F. L. Hernando, Microglial immune response is impaired against the neurotropic fungus Lomentospora prolificans. *Cell Microbiol.* **20**, e12847 (2018).

72. H. Keren-Shaul, A. Spinrad, A. Weiner, O. Matcovitch-Natan, R. Dvir-Szternfeld, T. K. Ulland, E. David, K. Baruch, D. Lara-Astaiso, B. Toth, S. Itzkovitz, M. Colonna, M. Schwartz, I. Amit, A unique microglia type associated with restricting development of alzheimer's disease. *Cell* **169**, 1276–1290.e17 (2017).

73. Y. Wang, X. Zhang, Q. Song, Y. Hou, J. Liu, Y. Sun, P. Wang, Characterization of the chromatin accessibility in an Alzheimer's disease (AD) mouse model. *Alzheimers Res. Ther.* **12**, 29 (2020).

74. J. V. Haure-Mirande, M. Wang, M. Audrain, T. Fanutza, S. H. Kim, S. Heja, B. Readhead, J. T. Dudley, R. D. Blitzer, E. E. Schadt, B. Zhang, S. Gandy, M. E. Ehrlich, Correction: Integrative approach to sporadic Alzheimer's disease: Deficiency of TYROBP in cerebral Aβ amyloidosis mouse normalizes clinical phenotype and complement subnetwork molecular pathology without reducing Aβ burden. *Mol. Psychiatry* **24**, 472 (2019).

75. H. S. Yang, K. D. Onos, K. Choi, K. J. Keezer, D. A. Skelly, G. W. Carter, G. R. Howell, Natural genetic variation determines microglia heterogeneity in wild-derived mouse models of Alzheimer's disease. *Cell Rep.* **34**, 108739 (2021).

76. U. Eyo, A. V. Molofsky, Defining microglial-synapse interactions. *Science* **381**, 1155–1156 (2023).

77. T. K. Lim, E. S. Ruthazer, Microglial trogocytosis and the complement system regulate axonal pruning in vivo. *Elife* **10**, (2021).

78. M. E. Price, B. A. McCool, Chronic alcohol dysregulates glutamatergic function in the basolateral amygdala in a projection-and sex-specific manner. *Front. Cell Neurosci.* **16**, 857550 (2022).

79. S. Zhao, A. D. Umpierre, L. J. Wu, Tuning neural circuits and behaviors by microglia in the adult brain. *Trends Neurosci.* **47**, 181–194 (2024).

80. M. A. S. Khan, S. L. Chang, Alcohol and the brain-gut axis: The involvement of microglia and enteric glia in the process of neuro-enteric inflammation. *Cells* **12**, 2475 (2023).

81. P. Mews, G. Egervari, R. Nativio, S. Sidoli, G. Donahue, S. I. Lombroso, D. C. Alexander, S. L. Riesche, E. A. Heller, E. J. Nestler, B. A. Garcia, S. L. Berger, Alcohol metabolism contributes to brain histone acetylation. *Nature* **574**, 717–721 (2019).

82. J. A. Pasman, K. J. H. Verweij, J. M. Vink, Systematic review of polygenic gene-environment interaction in tobacco, alcohol, and cannabis use. *Behav. Genet.* **49**, 349–365 (2019).

83. K. G. Chartier, K. J. Karriker-Jaffe, C. R. Cummings, K. S. Kendler, Review: Environmental influences on alcohol use: Informing research on the joint effects of genes and the environment in diverse U.S. populations. *Am. J. Addict* **26**, 446–460 (2017).

84. *Diagnostic and statistical manual of mental disorders: DSM-5™* (American Psychiatric Publishing Inc., ed. 5, 2013), 947 pp.

85. M. Jin, R. Xu, L. Wang, M. M. Alam, Z. Ma, S. Zhu, A. C. Martini, A. Jadali, M. Bernabucci, P. Xie, K. Y. Kwan, Z. P. Pang, E. Head, Y. Liu, R. P. Hart, P. Jiang, Type-I-interferon signaling drives microglial dysfunction and senescence in human iPSC models of Down syndrome and Alzheimer's disease. *Cell Stem Cell* **29**, 1135–1153.e8 (2022).

86. A. Maximov, Z. P. Pang, D. G. Tervo, T. C. Südhof, Monitoring synaptic transmission in primary neuronal cultures using local extracellular stimulation. *J. Neurosci. Methods* **161**, 75–87 (2007).

87. E. N. Oni, A. Halikere, G. Li, A. J. Toro-Ramos, M. R. Swerdel, J. L. Verpeut, J. C. Moore, N. T. Bello, L. J. Bierut, A. Goate, J. A. Tischfield, Z. P. Pang, R. P. Hart, Increased nicotine response in iPSC-derived human neurons carrying the CHRNA5 N398 allele. *Sci. Rep.* **6**, 34341 (2016).

88. L. Wang, V. R. Mirabella, R. Dai, X. Su, R. Xu, A. Jadali, M. Bernabucci, I. Singh, Y. Chen, J. Tian, P. Jiang, K. Y. Kwan, C. Pak, C. Liu, D. Comoletti, R. P. Hart, C. Chen, T. C. Südhof, Z. P. Pang, Analyses of the autism-associated neuroligin-3 R451C mutation in human neurons reveal a gain-of-function synaptic mechanism. *Mol. Psychiatry* **29**, 1620–1635 (2022).

89. M. S. Scarnati, A. J. Boreland, M. Joel, R. P. Hart, Z. P. Pang, Differential sensitivity of human neurons carrying mu opioid receptor (MOR) N40D variants in response to ethanol. *Alcohol* **87**, 97–109 (2020).

90. Y. Guo, Y. Chen, S. Carreon, M. Qiang, Chronic intermittent ethanol exposure and its removal induce a different miRNA expression pattern in primary cortical neuronal cultures. *Alcohol Clin. Exp. Res.* **36**, 1058–1066 (2012).

91. R. Lieberman, E. S. Levine, H. R. Kranzler, C. Abreu, J. Covault, Pilot study of iPS-derived neural cells to examine biologic effects of alcohol on human neurons in vitro. *Alcohol Clin. Exp. Res.* **36**, 1678–1687 (2012).

92. M. S. Scarnati, A. J. Boreland, M. Joel, R. P. Hart, Z. P. Pang, Differential sensitivity of human neurons carrying μ opioid receptor (MOR) N40D variants in response to ethanol. *Alcohol* **87**, 97–109 (2020).

93. K. Young, H. Morrison, Quantifying microglia morphology from photomicrographs of immunohistochemistry prepared tissue using ImageJ. *J. Vis. Exp.* **136**, 57648 (2018).

94. A. Karperien, H. Ahammer, H. F. Jelinek, Quantitating the subtleties of microglial morphology with fractal analysis. *Front. Cell Neurosci.* **7**, 3 (2013).

95. M. D. M. Fernandez-Arjona, J. M. Grondona, P. Granados-Duran, P. Fernandez-Llebrez, M. D. Lopez-Avalos, Microglia morphological categorization in a rat model of neuroinflammation by hierarchical cluster and principal components analysis. *Front Cell Neurosci* **11**, 235 (2017).

96. A. Mortazavi, B. A. Williams, K. McCue, L. Schaeffer, B. Wold, Mapping and quantifying mammalian transcriptomes by RNA-Seq. *Nat. Methods* **5**, 621–628 (2008).

97. A. Halikere, D. Popova, M. S. Scarnati, A. Hamod, M. R. Swerdel, J. C. Moore, J. A. Tischfield, R. P. Hart, Z. P. Pang, Addiction associated N40D mu-opioid receptor variant modulates synaptic function in human neurons. *Mol. Psychiatry* **25**, 1406–1419 (2020).

98. M. E. Ritchie, B. Phipson, D. Wu, Y. Hu, C. W. Law, W. Shi, G. K. Smyth, limma powers differential expression analyses for RNA-sequencing and microarray studies. *Nucleic Acids Res.* **43**, e47 (2015).

99. C. W. Law, Y. Chen, W. Shi, G. K. Smyth, voom: Precision weights unlock linear model analysis tools for RNA-seq read counts. *Genome Biol.* **15**, R29 (2014).

100. W. S. Cleveland, Robust locally weighted regression and smoothing scatterplots. *J. Am. Stat. Assoc.* **74**, 829–836 (1979).

101. G. Yu, L. G. Wang, Y. Han, Q. Y. He, clusterProfiler: An R package for comparing biological themes among gene clusters. *Omics* **16**, 284–287 (2012).

102. Y. Hao, S. Hao, E. Andersen-Nissen, W. M. Mauck, 3rd, S. Zheng, A. Butler, M. J. Lee, A. J. Wilk, C. Darby, M. Zager, P. Hoffman, M. Stoeckius, E. Papalexi, E. P. Mimitou, J. Jain, A. Srivastava, T. Stuart, L. M. Fleming, B. Yeung, A. J. Rogers, J. M. McElrath, C. A. Blish, R. Gottardo, P. Smibert, R. Satija, Integrated analysis of multimodal single-cell data. *Cell* **184**, 3573–3587.e29 (2021).